Synthesis of Reactive Crystallization Processes

David A. Berry and Ka M. Ng
Dept. of Chemical Engineering, University of Massachusetts, Amherst, MA 01003

A systematic method is presented to synthesize reactive crystallization processes. It shows how to selectively crystallize a desired solid product(s) after a reaction step and how to use compound formation to effect separation of a mixture. The method is based on the generation of phase diagrams with liquid-phase reactions. Using transformed coordinates, systems with three or fewer degrees of freedom can be conveniently analyzed, regardless of the number of components and reactions. Features of the solid–liquid phase diagram that are relevant to process synthesis are identified. The method is illustrated with systems with multiple components, complex reactions, and multiple phases.

Introduction

Myriads of basic chemicals, agricultural products, pharmaceuticals, pigments, and ceramic powders are produced by reactive crystallization-based processes. An example is the liquid-phase air oxidation of *p*-xylene to produce technical-grade terephthalic acid. In this process, the solvent, acetic acid, is condensed and refluxed to remove the heat of reaction. The yield in the form of crystals is often in excess of 90 mol % because the terephthalic acid dissolves to a limited extent in the acetic acid (Bemis et al., 1982).

Reactions are also utilized for separations that conventional methods cannot normally accomplish. In adductive crystallization processes, the solid reaction products are remelted and distilled into pure species. In the resin-catalyzed process for production of bisphenol A, the crude product is purified by means of an adductive crystallization step (Mendiratta, 1983). The use of urea and thiourea complexes is used in several commercial processes to dewax oils and to recover *n*-paraffins from heavy gas oils (Dale, 1981). Other potential applications have also been reported in the literature. For example, Lahti and Manning (1965) and Bailey et al. (1951) investigated the use of urea to crystallize straight-chain hydrocarbons. McCandless et al. (1972, 1973) reported the separation of trimethylpentanes and β-phellandrene from dipentene with thiourea.

Gaikar and Sharma (1987) and Gaikar et al. (1989) proposed a novel separation process that they coined dissociation extractive crystallization. These separations are based on the complexation chemistry of weak acids and bases with a neutralizing agent. These processes often involve aqueous-organic liquid-phase splits. They studied the separation of 2,6-xylenol/*p*-cresol, piperazine/*M*-methylpiperazine, *N*-methylpiperazine/*N*,*N*′-dimethylpiperazine, *N*-alkyl-substituted anilines, *o*-/*p*-chloroanilines, among others.

Due to the great importance of reactive crystallization, much research has focused on understanding the underlying phenomena affecting these processes. The studies have concentrated on two major issues: measurement of kinetic parameters and simulation of reactor performance to determine the effects of operating conditions on crystal size distribution and reaction selectivity. For example, Momonaga and Yazawa (1992) deduced the reaction kinetics, measured the crystal size distribution, and proposed a method for crystallizer scale-up for the production of methyl α-methoxyimino acetoacetate. Toyokura et al. (1979) reported producing crystals of sulfamic acid by reaction of urea and fuming sulfuric acid.

The most scrutiny has been placed on systems with fast chemical reactions. Tavare and Gaikar (1991) modeled the precipitation of salicylic acid from hydrotropic solutions by using either water or dilute hydrosulfuric acid as a drowning-out agent. Åslund and Rasmuson (1992) experimentally determined the effects of incomplete mixing and of the mode of feeding reactants on the performance of a semibatch reactor to produce particles of benzoic acid. Söhnel and Garside (1992) described the fundamentals and practical issues related to precipitation processes. Mersmann and Kind (1988) reviewed chemical engineering aspects of precipitation from solution. Franke and Mersmann (1995) investigated the influence of operating conditions on the precipitation of calcium sulfate. Franck et al. (1988) modeled the batch kinetics of

Correspondence concerning this article should be addressed to K. M. Ng.

salicylic acid. Marcant and David (1991) provided predictions and experimental evidence for micromixing effects in precipitation processes. Tavare (1995) discussed the difficulties encountered when modeling mixing in precipitation reactors.

Contrary to all this detailed work, systematic methods for synthesizing reactive crystallization processes are not as well developed. The method must identify desirable reaction conditions, process alternatives, process limitations, and design variables. Recently, the conceptual design of other crystallization-based separation processes has been receiving much attention. Söhnel (1991) and Lencka and Riman (1993) used precipitation diagrams to determine the effects of pH, temperature, and concentration on the species crystallizing. Rajagopal et al. (1991) and Dye and Ng (1995a) used phase diagrams to design extractive crystallization processes to completely separate binary and ternary systems, respectively. A similar approach was taken for the design of fractional crystallization processes (Rajagopal et al., 1988; Dye and Ng, 1995b; Berry and Ng, 1996). Berry et al. (1996) provided a systematic method to design drowning-out crystallization-based separation processes.

In this article we propose a method to synthesize reactive crystallization processes. The article is divided into three sections. The first section describes reactive phase equilibrium calculations and reviews a coordinate transform used to plot phase diagrams. The second section analyzes several examples of heterogeneous phase diagrams of multicomponent reactive systems. This section is geared to identifying reaction conditions that cause the selective crystallization of specific components. The third section illustrates how to synthesize processes to separate pure components from reactive mixtures. Examples are given that utilize temperature swings, pressure swings, and evaporation.

Description of Solid–Liquid Phase Diagrams for Systems with Reactions

There is an abundance of systems with reactions from which crystallization can occur. Ionic and molecular compounds have been precipitated to form powders and pigments (Schiek, 1982). Processes have been proposed that use adducts, clathrates, and Werner complexes to separate one or more components from solution (Dale, 1981). Chelates are often used in electrochemical processes to increase the solubility of metallic species in aqueous solutions (McCrary and Howard, 1979).

Table 1 provides a list of examples for systems with reactions that may lead to solidification. We do not attempt to generate the phase diagrams of any of these systems because much of the required information is unavailable. Instead, this article presents several hypothetical phase diagrams of increasing complexity. Features of the phase diagrams that can be exploited to synthesize novel or improved separation processes are identified. Also, a better understanding of these diagrams is expected to help efforts in data collection and correlation.

Generation of solid–liquid phase diagrams for systems with reactions

The Gibbs phase rule for a reactive mixture at equilibrium can be written as

$$f = c - p - r + 2, \tag{1}$$

where f is the degrees of freedom, c the number of components, p the number of phases, and r the number of inde-

Table 1. Examples of Multiphase Reactive Systems with 1, 2 and 3 Deg of Freedom*

Systems with one degree of freedom:
$A + 3B \rightarrow C + 2D$ (Bemis et al., 1982)
I
A = p-xylene (l, g), $B = O_2$ (l, g), C = terephthalic acid (l, s), $D = H_2O$ (l, g), I = acetic acid (l, g)
$A + B + C \rightarrow 2D + E$ (Toyokura et al., 1979)
$A = NH_3CONH_2$ (l), $B = SO_3$ (l), $C = H_2SO_4$ (l), $D = NH_3SO_3H$ (s), $E = CO_2$(g)
$A + B \rightarrow C + 2D$ (Mersmann and Kind, 1988)
$A = Ba(OH)_2$ (l), $B = H_2SO_4$ (l), $C = BaSO_4$ (l,s), $D = H_2O$ (l)
Systems with two degrees of freedom:
$A + 2B \rightarrow C + D$ (Schiek, 1982)
$4C + E \rightarrow 2F + 2G$
$4A + 6G + E \rightarrow 2F + 4H$
$A = FeSO_4$ (l), $B = NaOH$ (l), $C = Fe(OH)_2$ (l), $D = Na_2SO_4$ (l),
$E = O_2$ (l, g), $F = Fe_2O_3 \cdot H_2O$ (l, s), $G = H_2O$ (l), $H = H_2SO_4$ (l)
$A + B \rightarrow C + D$ (Schiek, 1982)
I
$A = ZnSO_4$ (l), $B = BaS$ (l), $C = ZnS$ (s, l), $D = BaSO_4$ (l), $I = H_2O$ (l)
Systems with six degrees of freedom:
$A + 2B + C \rightarrow D + E + 2F$ (Momonaga et al., 1992)
$2D + G + 2H \rightarrow 2I + J + 2K$
A = MA (l1), $B = NaNO_2$ (l1,l3), $C = H_2SO_4$ (l1), D = OX (l1), $E = Na_2SO_4$ (l1,l3),
$F = H_2O$, $G = (CH_3)_2SO_4$ (l2,l3), $H = K_2CO_3$ (l1,l3), I = MME (s,l3), $J = K_2SO_4$ (l1,l3),
$K = KHCO_3$
where MA = methyl acetoacetate and MME = methyl α-methoxyimino acetate;
OX = oxime; and l1, l2, l3 represent the three liquid phases.

*The degrees of freedom are calculated by assuming that the temperature and the pressure are specified and that crystals precipitate from a solution phase. Phases of the reactants are given by (g) for gas, (s) for solid, and (l) for liquid.

pendent reactions. For each of the r reactions in Eq. 1, there is an equilibrium constant, K_R, which can be written as

$$K_R = \exp\left(\frac{-\Delta G_R}{RT}\right), \tag{2}$$

where ΔG_R is the standard Gibbs free energy of reaction R, R is the gas constant, and T is the temperature. The equilibrium constant is related to the mole fractions of species by

$$K_R = \prod_{i=1}^{c} (x_{i,eq}\gamma_i)^{\nu_{i,R}}, \tag{3}$$

where $x_{i,eq}$ and γ_i are the equilibrium composition and activity coefficient of component i, respectively. The stoichiometric coefficient for component i in reaction R is given by $\nu_{i,R}$. The composition of component i must be less than or equal to its saturation composition. When contribution of the change in the heat capacity due to melting is small and the solid phases are completely immiscible, the saturation composition is given by the melting surface equation:

$$x_i^{\text{sat}} = \frac{1}{\gamma_i}\exp\left[\frac{\Delta H_{m,i}^0}{R}\left(\frac{1}{T_{m,i}} - \frac{1}{T}\right)\right], \tag{4}$$

where ΔH_m^0 is the heat of melting, and T_m the melting temperature. The liquid-phase activity coefficient can be calculated with various models such as the two-suffix Margules equation (Malesinski, 1965), among others. Notice that for ideal systems, the solubility of component i is a function of only temperature.

Equations 1 through 4 provide the basis from which solid–liquid phase diagrams can be calculated. The following algorithm can be used to calculate solid–liquid phase diagrams with reactions for condensed systems with a single-liquid phase:

(i) Specify values for T and P.

(ii) Choose k component(s) to be saturated. The number of equilibrium phases must not violate the phase rule, Eq. 1.

(iii) Initialize γ_i, $i = 1, 2, \ldots, c$.

(iv) Calculate K_R, $R = 1, 2 \ldots, r$ by Eq. 2.

(v) Choose values less than x_j^{sat} for the remaining $(c\text{-}r\text{-}k)$ compositions.

(vi) Calculate the saturation composition of the k solids by Eq. 4.

(vii) Calculate remaining r compositions with Eq. 3.

(viii) Note that the sum of the mole fractions must add up to unity.

(ix) Calculate γ_i, $i = 1, 2, \ldots, c$.

(x) Repeat (vi)–(ix) until the latest estimate of mole fractions equal their previous values.

(xi) If the solution indicates that the specified solids cannot coexist, or one or more of the $c-k$ components are saturated, there are three options. One, make a new guess for the values of the unsaturated components and then go to step (v). Two, choose a different set of k solids and go to step (iii). Three, specify a new temperature and go to step (ii).

(xii) Accept point.

(xiii) Repeat entire algorithm with a new temperature, a different set of k components, or with new values of x_j so that saturation boundaries of the k components are clearly designated.

While this algorithm can only be used to calculate molecular solid–liquid phase diagrams, it is provided to give a framework from which more general algorithms can be developed for more complicated systems. In particular, when a vapor phase or a liquid–liquid split are present, additional equations can be readily included to describe the composition of the additional phases. When the species dissociate, as do salts, acids, and bases, the system must also satisfy a charge balance. The solubility of salts is often expressed in terms of solubility products, and Eq. 4 is no longer valid. For more general algorithms to calculate phase equilibrium, see Prausnitz et al. (1986) and Smith and Missen (1982).

Coordinate transform used to plot multicomponent phase diagrams

The solid–liquid phase diagram of a system with reactions can be plotted once the compositions of the saturation boundaries are calculated. Although the phase diagrams can be plotted in mole-fraction coordinates, this representation of multicomponent phase diagrams has two major drawbacks. First, only diagrams with three or fewer components are easily represented in mole-fraction coordinates. Second, reactions constrain the system to compositions that lie on a reaction surface. As a result, many regions in composition space do not represent equilibrium compositions.

A coordinate system can be chosen so that all the compositions shown in a phase diagram are those on a reaction surface. Using this transformed coordinate system also reduces the number of independent coordinates by the number of reactions without loss of any information from a phase diagram plotted in mole-fraction coordinates. Phase diagrams of multicomponent systems with three or fewer degrees of freedom can easily be plotted, regardless of the number of components or the number of reactions.

Ung and Doherty (1995) provided a general transform to plot multicomponent vapor–liquid phase diagrams of reacting systems. The transform was also used by Slaughter and Doherty (1995) to plot binary solid–liquid phase diagrams for systems that undergo solid-phase reactions to form compounds. We apply the same transform to multicomponent systems with multiple solid and liquid phases, and with multiple liquid-phase reactions to analyze features of composition space that can be utilized to synthesize crystallization-based separation processes. In addition, with a minor extension to the transform, information on the dissolution of solids can be obtained.

The transform can be derived in the following manner. Consider a system of r independent reactions among c reacting components. The chemical reactions can be represented in the following way:

$$\nu_{1R}A_1 + \nu_{2R}A_2 + \cdots + \nu_{cR}A_c = 0 \qquad R = 1, 2, \ldots, r, \tag{5}$$

where A_i are the reacting species, and ν_{iR} is the stoichiometric coefficient of component i in reaction R. By convention $\nu_{iR} < 0$ if component i is a reactant in reaction R, $\nu_{iR} > 0$ if component i is a product, and $\nu_{iR} = 0$ if component i does not participate in reaction R. Using vector-matrix formalism, the following vectors are defined:

$$\boldsymbol{\nu}_i^T = (\nu_{i1}, \nu_{i2}, \ldots, \nu_{ir}) \tag{6}$$

$$\boldsymbol{\nu}_{TOT}^T = (\nu_{TOT1}, \nu_{TOT2}, \ldots, \nu_{TOTr}), \tag{7}$$

where $\boldsymbol{\nu}_i^T$ is the row vector of stoichiometric coefficients of component i in each reaction and $\boldsymbol{\nu}_{TOT}^T$ is the row vector of the sum of the stoichiometric coefficients for each reaction. At any instant, the mole fraction of component i, x_i, can be expressed as

$$x_i = \frac{x_i^0 + \boldsymbol{\nu}_i^T \boldsymbol{\xi}}{1 + \boldsymbol{\nu}_{TOT}^T \boldsymbol{\xi}} \qquad i = 1, \ldots, c, \tag{8}$$

where x_i^0 is the initial mole fraction of component i and $\boldsymbol{\xi}$ is the column vector of the r dimensionless extents of reaction

$$\boldsymbol{\xi} = (\xi_1, \xi_2, \ldots, \xi_r)^T. \tag{9}$$

The r extents of reaction are eliminated from these c equations by choosing a subsystem of r equations from Eq. 8. The r components chosen to eliminate the r extents of reaction are called the reference components, thus:

$$\boldsymbol{x}_{\text{ref}} = \frac{\boldsymbol{x}_{\text{ref}}^0 + V\boldsymbol{\xi}}{1 + \boldsymbol{\nu}_{TOT}^T \boldsymbol{\xi}}, \tag{10}$$

where $\boldsymbol{x}_{\text{ref}}$ is the column vector composed of the mole fractions of the r reference components, $\boldsymbol{x}_{\text{ref}}^0$ is the column vector of the initial mole fractions of the r reference components, and V is the square matrix of stoichiometric coefficients for the r reference components in the r reactions, or

$$\boldsymbol{x}_{\text{ref}} = (x_{(c-r+1)}, x_{(c-r+2)}, \ldots, x_c)^T \tag{11}$$

$$\boldsymbol{x}_{\text{ref}}^0 = \left(x_{(c-r+1)}^0, x_{(c-r+2)}^0, \ldots, x_c^0\right)^T \tag{12}$$

$$V = \begin{pmatrix} \nu_{(c-r+1)1} & \cdots & \nu_{(c-r+1)r} \\ \cdots & \nu_{ir} & \cdots \\ \nu_{c1} & \cdots & \nu_{cr} \end{pmatrix}. \tag{13}$$

By substituting $\boldsymbol{\xi}$ from Eq. 10 into Eq. 8, one obtains the following transformed set of coordinates

$$X_i = \frac{x_i^0 - \boldsymbol{\nu}_i^T V^{-1} \boldsymbol{x}_{\text{ref}}^0}{1 - \boldsymbol{\nu}_{TOT}^T V^{-1} \boldsymbol{x}_{\text{ref}}^0} = \frac{x_i - \boldsymbol{\nu}_i^T V^{-1} \boldsymbol{x}_{\text{ref}}}{1 - \boldsymbol{\nu}_{TOT}^T V^{-1} \boldsymbol{x}_{\text{ref}}} \qquad i = 1, \ldots, c\text{-}r. \tag{14}$$

The $(c\text{-}r)$ transforms possess two convenient properties. First, they sum to unity; second, the transformed variables are reaction-invariant, or

$$X_i(\mathbf{0}) = X_i(\boldsymbol{\xi}) \qquad \forall \boldsymbol{\xi} \qquad i = 1, \ldots, c\text{-}r. \tag{15}$$

This means that the transformed coordinates describe the system as if no reactions were occurring at all. Thus, the transformed coordinate system can be applied to both equilibrium constrained and to kinetically controlled reactions.

The transform can be used to represent equilibrium conditions or conditions where a solid dissolves. To represent equilibrium conditions, the value of x_i in Eq. 14 is allowed to vary between 0 and x_i^{sat}. After plotting the compositions where x_i equals x_i^{sat}, the compositions where component i is unsaturated can clearly be determined. To represent nonequilibrium conditions where a solid dissolves, x_i is set to x_i^{sat}. The mole fractions of the other c-1 components can be no greater than their saturation values. Use of the transforms in this manner projects the entire melting surface of component i onto the phase diagram, and thus shows some compositions that do not satisfy reaction equilibria. This representation shows values of X_i where solid i dissolves and the values where reaction and phase equilibrium are simultaneously satisfied. Examples of phase diagrams that use both methods are given in the following section.

Examples of Solid–Liquid Phase Diagrams with Reactions

Phase diagrams for five systems are given. The first system is composed of three components and undergoes one reaction. Both the polythermal and isothermal phase diagrams are given. The transformed isothermal phase diagram is contrasted to the same diagram plotted in mole-fraction coordinates. Examples are given for high and intermediate melting compounds. The second system is a quaternary mixture where one of the components is an inert liquid. The phase diagram in mole fraction coordinates is contrasted to one in the transformed coordinates and also to the phase diagram without inert. The third example is a quaternary, isothermal, isobaric system where multiple solids can crystallize. Compositions are identified that lead to selective crystallization and to cocrystallization. The fourth system consists of gaseous, liquid, and solid phases. Conditions where one component crystallizes over a range of compositions are identified. The fifth example is a seven-component system that also undergoes a liquid–liquid phase split and two reactions.

Condensed, ternary system with one reaction

Consider a system composed of components A, B, and C that undergoes the following reaction:

$$A + B \leftrightarrow C\downarrow, \tag{16}$$

where C has limited solubility in the solution. Since the phase and reaction equilibrium can be decoupled, we first consider the effects of the reactions on the phase diagram. Assuming that the system is condensed and that temperature is specified, Eq. 1 indicates that the system possesses one degree of freedom. This means that the equilibrium compositions are constrained to lie on a line. Figure 1 is the phase diagram for this ideal system, with $K = 1$, 10, and 100. The dashes are lines of constant stoichiometry and can be calculated from

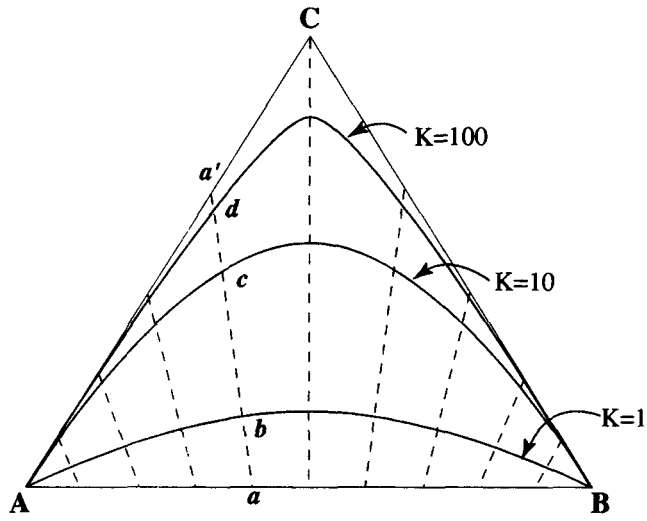

Figure 1. Homogeneous phase diagram with various reaction equilibrium constants for $A+B \leftrightarrow C$.

Eq. 8. Given an initial composition, the final composition of the system can be found by the point of intersection between a line of constant stoichiometry and a solution to Eq. 3. For example, the final composition of a solution with an initial composition on line aa' is point b, c, or d for $K = 1$, 10, and 100, respectively. If the initial composition of the solution lies above the equilibrium curve, C is consumed to produce equimolar amounts of A and B. If the initial composition of the solution lies below the equilibrium curve, A and B are consumed to produce C.

Equilibrating solid C with solution reduces the degrees of freedom by one and makes the system invariant. Figure 2 shows the complete phase diagram for this system for $K = 10$ and $x_C^{sat} = 0.5$. Both points 2 and 4 satisfy Eq. 3 and $x_C = x_C^{sat}$. Triangle $1C5$ represents the compositions saturated with C. Line 15 gives the solubility of C at all solution compositions. Points 1 and 5 are the solubility of C in A and B, respectively. If the solution were nonideal, the solubility of C would become a function of composition as well as temperature. The solubility in A and B would differ and line 15 would become curved. Curve $A6B$ represents the compositions that describe the reaction equilibrium. The portions of $A6B$ given by curves $A2$ and $B4$ represent compositions where C is unsaturated. The region 2346 represents the envelope formed by the intersection of the compositions saturated with C and the compositions with reaction equilibrium. Such envelopes are required for a reaction to produce a precipitate.

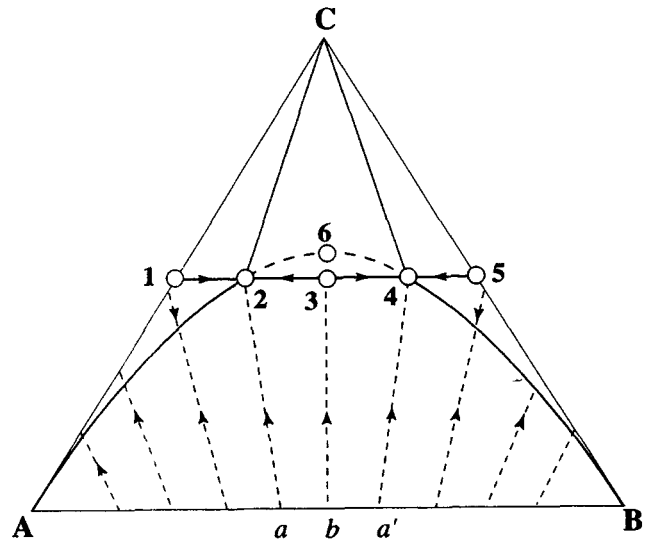

Figure 2. Heterogeneous phase diagram for $A+B \leftrightarrow C(s)$.

The system will remain unsaturated, become saturated, or digest C depending on the overall initial composition. A mixture within the region $12C$ ($54C$) will digest solid C because the composition lies above the reaction equilibrium curve. The composition of the solution moves along line 13 (53) until reaching point 2 (4). Mixtures with compositions within quadrilateral $Aa21$ ($Ba'45$) remain unsaturated with C. Mixtures within region $a23b$ ($a'43b$) move up along the lines of constant stoichiometry until becoming saturated with C. When C reaches it solubility limit, it crystallizes and the composition of the solution moves along curve 32 (34) until reaching point 2 (4). A mixture within region $2C3$ ($4C3$) will crystallize C because the composition of the solution lies below the reaction equilibrium curve. Crystallization continues until the composition moves to point 2 (4). Point 3 is saddle point. If the initial composition is at this point, there will be complete conversion to solid C. The yield increases the closer the initial conditions are to a line of constant stoichiometry which passes through point 3.

The phase diagram can also be plotted in the transformed coordinates. Using x_C as the reference component, the transformed coordinates are

$$X_A = \frac{x_A + x_C}{1 + x_C} \tag{17}$$

$$X_B = \frac{x_B + x_C}{1 + x_C}. \tag{18}$$

Since the system has zero degrees of freedom when the temperature and pressure are specified and when one solid equilibrates with solution, the phase diagram for this system is constrained to lie on a line in the transformed coordinate system. Figure 3 plots transformed phase diagrams and shows crystallization paths that describe the precipitation and the dissolution of C. Points on the phase diagram correspond to the same points on the phase diagram plotted in mole percent (Figure 2). The coordinates of pure component i are found by letting the mole fraction of i go to unity while the mole fractions of all the other components go to zero. These points are then plotted on the transformed phase diagram. Crystallization and dissolution paths of a pure solid may be generated by drawing a line through a given point and the point on the phase diagram that represents the respective pure component. The composition moves away from the coordinates of the pure component when the component crystallizes. The system moves toward the point when the component dissolves.

There are two ways to plot the phase diagram. The first view is shown in Figure 3a. This phase diagram shows the pure A, B, and C locations along the coordinate axis and

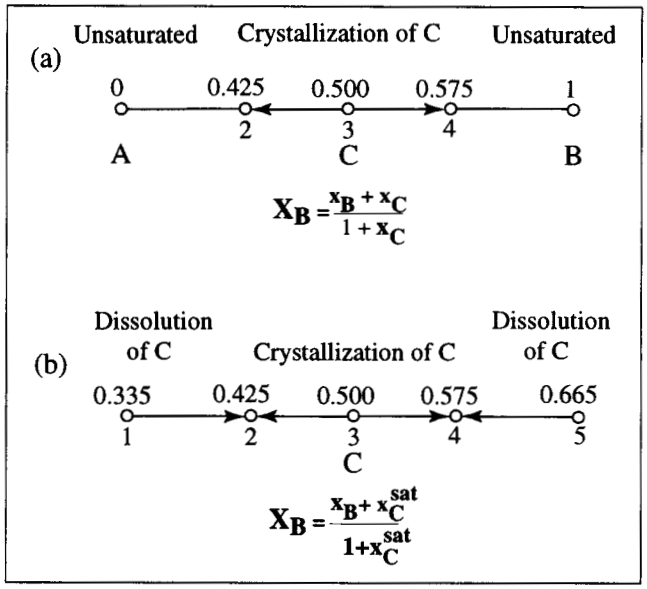

Figure 3. Heterogeneous phase diagram for $A + B \leftrightarrow C(s)$ in transformed coordinates.

indicates where C crystallizes and where the system is unsaturated. From $0 \le X_B < 0.425$ and from $0.575 < X_B \le 1$ the system remains unsaturated with respect to C. The equilibrium compositions are where X_B equals 0.425, 0.500, and 0.575. From $0.425 \le X_B < 0.5$ and $0.5 < X_B \le 0.575$, C precipitates until reaching point 2 or 4, respectively.

The second view is shown in Figure 3b. The entire C melting surface is projected onto the transform. This is accomplished by requiring $x_C = x_C^{sat}$ at all compositions on the phase diagram. This representation shows the coordinates over which C dissolves and the coordinates over which C crystallizes. The pure component locations for A and B are not shown in this representation. From $0.335 \le X_B < 0.425$ and $0.575 < X_B \le 0.665$, C dissolves until reaching points 4 or 2, respectively. The equilibrium compositions and the compositions where C crystallizes are identical to those presented for Figure 3a.

The phase diagrams given earlier are for the reaction of two low melting species to form a higher melting compound. A more common example would be the formation of an intermediate melting compound. Many such examples are found in systems that form hydrates and adducts. Table 2 gives several samples.

Figure 4 shows the polythermal phase diagram in the transformed coordinates as well as isothermal cuts for a system that forms an intermediate melting compound with 1:1 stoichiometry. Table 3 gives the physical parameters of the system. Below the transformed phase diagram are sketches of isothermal cuts of the phase diagram in mole-fraction coordinates. Notice that the melting temperature of C given in Table 3 is 305 K, but the phase diagram shows that C melts at 270 K. This observation can be explained by referring to the three isothermal cuts of the phase diagram that are plotted in mole-fraction coordinates. Begin at the 300 K isotherm. The dashed line represents the reaction equilibrium curve. Notice that the reaction line and A melting surface overlap. Component B is liquid at all compositions. There is a region on the phase diagram where C crystallizes; however, this region does not represent equilibrium compositions because the melting surface for C does not intersect with the reaction line. Crystals of C are not present at any composition at 300 K. The phase diagram shows that solution and solid A coexist. At 270 K the phase diagram consists of a region of homogeneous liquid and regions where A and solution, B and solution, and C and solution coexist. The melting surfaces for A and B overlap the reaction line when the temperature is lowered to 270 K. The reaction line is tangent to the C melting surface, which indicates that there is one composition where C solidifies. At 260 K the phase diagram consists of a region of liquid, a region where solids A and C coexist, and regions where B and solution and where C and solution coexist. Because the reaction occurs in the liquid phase, solids A and C do not react. The reaction line is not shown in this region.

Table 2. Examples of Species Forming Adducts

		$A + B = A \cdot B$	
A		B	Reference
Hydrazine		Water	Tyner (1955)
p-Cresol		2-Methyl-2-propanol	Jadhav et al. (1991)
Imidazole		Tetrazole	Hilgeman et al. (1989)
Quinaldine		Acetic acid	Tare and Chivate (1976a)
		$A + 2B = A \cdot 2B$	
A		B	Reference
Dioxane		Carbontetrachloride	Kennard and McCusker (1948)
Dioxane		Chloroform	Kennard and McCusker (1948)
		$A + 2B = A \cdot 2B$ $2A + B = 2A \cdot B$	
A		B	Reference
Phenol		2-Methyl-2-propanol	Jadhav et al. (1992)
		$A + B + C = A \cdot B \cdot C$	
A	B	C	Reference
p-Cresol	2,6-Xylenol	2-Methyl-2-propanol	Jadhav et al. (1991)
Quinaldine	Isoquinoline	Acetic acid	Tare and Chivate (1976b)
Phenol	*o*-Cresol	2-Methyl-2-propanol	Jadhav et al. (1992)

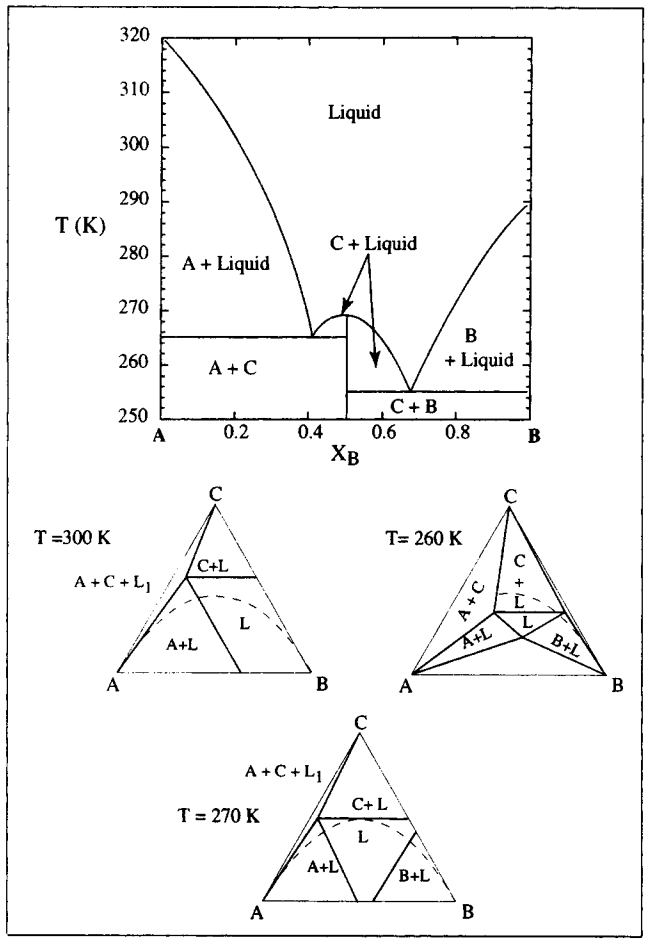

Figure 4. Polythermal phase diagram with the formation of an intermediate melting compound.

The melting temperature of C that is shown on the polythermal transformed phase diagram is the temperature where the C melting surface and the reaction line are tangent. In order to use the melting-surface equation, Eq. 4, to calculate the solubility of a compound, the melting temperature of pure C without reaction must be known. The melting temperature of C disregarding the reaction is the temperature at the C vertex as plotted on the polythermal, ternary phase diagram. This temperature can be calculated by replacing T in Eq. 4 with the melting temperature of C as read from the polythermal, transformed phase diagram (i.e., 270 K) and then solving for $T_{m,C}$.

Condensed, quaternary system with one reaction and an inert solvent

In many processes reactions take place in an inert component that serves as a diluent, drowning-out agent, or heat-transfer medium. The isobaric, isothermal phase diagram for reacting A with B to produce C in the presence of an inert, I, can be drawn as a regular tetrahedron in mole-fraction coordinates. Figure 5 is the diagram for $K = 10$ and $x_C^{sat} = 0.5$. Unshaded regions are unsaturated with respect to C. The lightly shaded region forms a tetrahedron that represents the conditions where C is supersaturated. Any composition on or within this region represents conditions where solid C equilibrates with solution. The darkly shaded surface represents the conditions that satisfy reaction equilibrium. The region where the saturation tetrahedron and the reaction surface intersect gives the compositions where the equations for phase and reaction equilibrium are simultaneously satisfied. Since the system has $4(c)-2(p)-1(r)=1$ degree of freedom under these conditions, the intersection is given by a curve.

Table 3. Parameters for System Producing 1:1 Compound in Figure 4

	ΔH_m^0 (J/mol)	T_m (K)	$K = 10$
A	10,000	320	
B	12,000	290	
C	14,000	305	

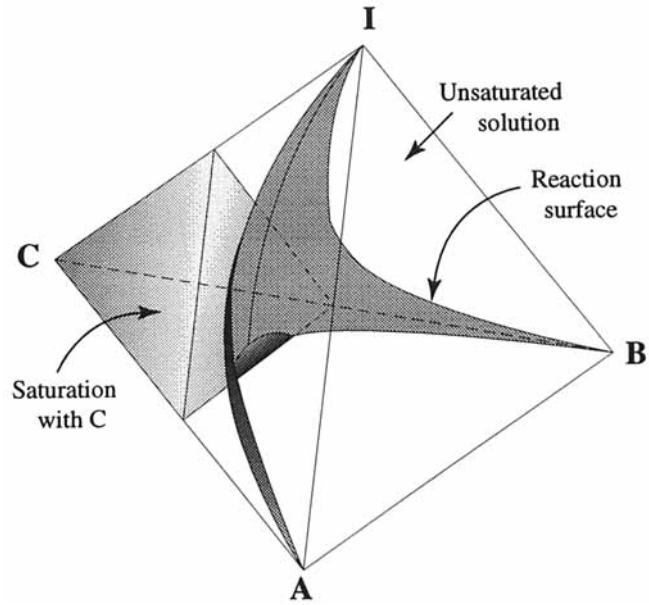

Figure 5. Phase diagram for $A + B \leftrightarrow C(s)$ in the presence of an inert I.

Identifying the compositions that satisfy both phase and reaction equilibrium from this phase diagram is awkward; however, the task is quite easy from diagrams plotted in the transformed coordinates. Taking C as the reference component gives the following coordinates:

$$X_A = \frac{x_A + x_C}{1 + x_C} \tag{19}$$

$$X_B = \frac{x_B + x_C}{1 + x_C} \tag{20}$$

$$X_I = \frac{x_I}{1 + x_C}. \tag{21}$$

Figure 6 is the transformed phase diagram that shows compositions where C dissolves and crystallizes. Curve 234 gives the equilibrium compositions where C equilibrates with solution. The region within $C234$ represents a supersaturated solution. A system at point a dissolves C to produce A and B and equilibrates at point b. A system at a point on the line between point C and point 3 converges to point 3.

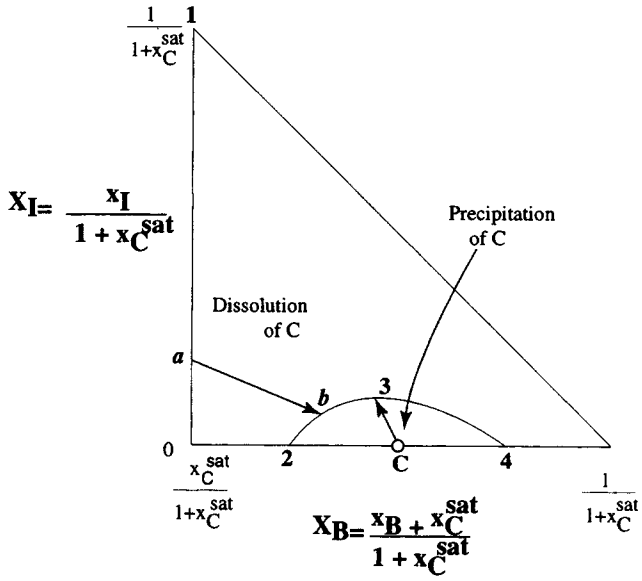

Figure 6. Phase diagram for $A + B \leftrightarrow C(s)$ in inert I in transformed coordinates.

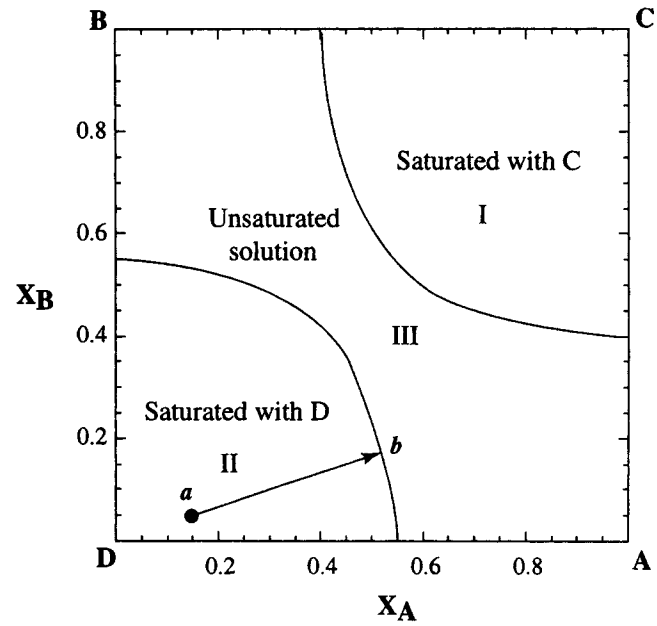

Figure 7. Phase diagram for $A + B \leftrightarrow C\downarrow + D\downarrow$.

Condensed quaternary system where reaction products can cocrystallize

In many reactive crystallization processes it is possible for more than one solid to crystallize. For example, consider the reaction under isobaric and isothermal conditions

$$A + B \leftrightarrow C\downarrow + D\downarrow \tag{22}$$

where C and D are partially insoluble. The phase diagram of this system in mole fraction coordinates can be represented as a tetrahedron. The unsaturated solution has two degrees of freedom. Regions where either C or D equilibrate with solution have one degree of freedom. Regions where C, D and solution equilibrate have zero degrees of freedom. Choosing C as the reference component gives the following independent transformed coordinates:

$$X_A = x_A + x_C \tag{23}$$

$$X_B = x_B + x_C. \tag{24}$$

Figure 7 is the phase diagram for x_C^{sat} and x_D^{sat} equal to 0.4 and 0.45, respectively, and K equal to 6. Points A, B, C, and D represent the pure components. There are three regions on the phase diagram. Region I is saturated with C; region II is saturated with D; region III is unsaturated solution. Any mixture with a composition within region I (II) will react and crystallize C (D). For example, consider point a. As D crystallizes, the composition of the system moves from point a to point b. Point b is a composition that satisfies both phase and reaction equilibrium and is the final composition of the system. Feed compositions within region III do not lead to crystallization. It is not possible to coprecipitate both C and D at this temperature.

Figure 8 is the phase diagram for K equal to 60. The solubility of C and D are identical to that given in the previous example. With the increase in K, the solubility curves touch to form the lightly shaded region $D1C3$. Any initial composition located within this region coprecipitates a mixture of C and D. Points 1 and 3 are the solutions to the simultaneous phase and reaction equilibrium for the presence of both C and D as solids. For example, consider an initial composition within region $D12$. Pure D crystallizes as the composition moves along the precipitation ray from D until the system reaches a point on 12. A mixture of C and D crystallizes as the system moves along 21 until reaching point 1. Like several of the earlier examples with molecular systems, a saddle point (point 2) exists where lines of constant stoichiometry and crystallization paths coincide. Any system that reaches point 2 crystallizes all the C and D from solution.

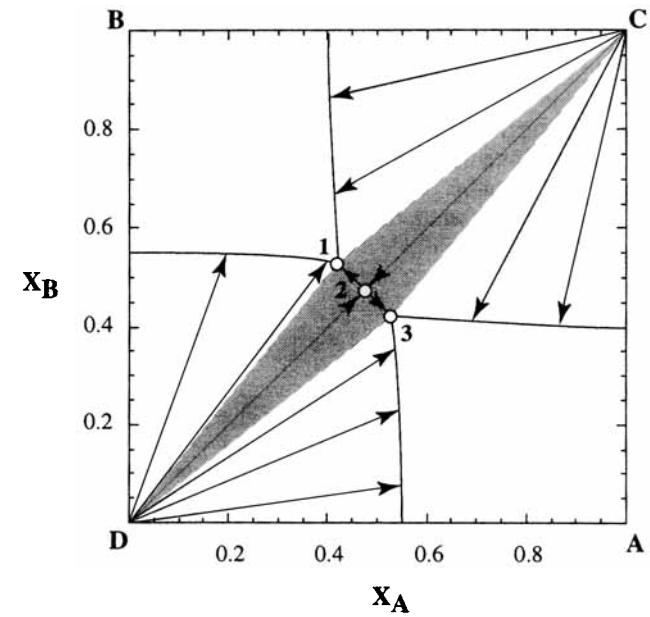

Figure 8. Phase diagram for $A + B \leftrightarrow C\downarrow + D\downarrow$, where C and D can cocrystallize.

Six-component vapor – liquid – solid system with two reactions

In the previous examples, the systems were assumed to be condensed. While this assumption simplifies calculations required to represent the reactive phase diagram, a vapor phase can have great impact on crystallizer operation. Control of the total pressure or the partial pressures of one or more components can often determine which component crystallizes. For example, species that can react with carbon dioxide in air may precipitate unwanted carbonates.

To demonstrate the need to consider the vapor phase over a solution from which crystallization is to take place, consider the following reactions in a volatile inert I:

$$A + B \leftrightarrow C \downarrow \tag{25}$$

$$A + D(g) \leftrightarrow E \downarrow \tag{26}$$

Both C and E have limited solubility in the solution. Component C is the desired product; component E is an unwanted byproduct. Gas I can be used to purge D to a lower vapor concentration and thus reduce the concentration of D in solution. The number of degrees of freedom where C equilibrates with solution and vapor is $6(c)-3(p)-2(r)=1$. The number of transformed variables is four. The temperature is fixed and pressure is 1 atm. Figure 9 shows the system in terms of X_A and X_B, and also in terms of X_D and X_I. Components C and E are chosen to be the reference components. The input parameters to generate the plot are given in Table 4. Compositions within region CL_11 and C_3L_11 split into solution and crystals of C. Compositions within EL_12 and EL_14 split into solution and crystals of E. Compositions within CEL_1 split into liquid $L1$ and crystals of C and E. The partial pressure of D was not plotted to maintain the clarity of the figure. Thus, this analysis clearly shows the conditions under which only C crystallizes.

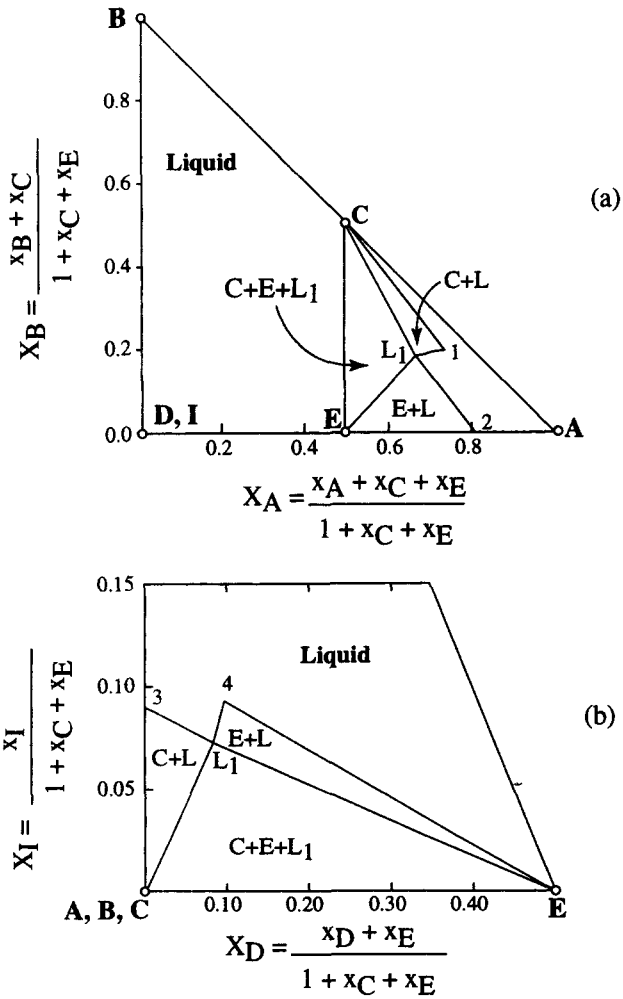

Figure 9. Phase diagram for a vapor–liquid–solid system with two reactions.

Table 4. Parameters to Generate the Vapor–Liquid–Solid Phase Diagram in Figure 9

$K1 = 10$	$K2 = 15$
$x_C^{sat} = 0.2$	$x_D^{sat} = 0.15$
$P_A^{sat} = 0.10$ atm	$P_D^{sat} = 10.0$ atm
$P_B^{sat} = 0.15$ atm	$P_E^{sat} = 0.001$ atm
$P_C^{sat} = 0.20$ atm	$P_I^{sat} = 8.2$ atm

Seven-component system with liquid – liquid phase split and two reactions

Reactive extractive crystallization is a novel separation technique that couples crystallization, reactions, and a liquid–liquid phase split. Although yield and selectivity are often very good, it is difficult to design such processes because they are multicomponent in nature. For example, consider a system composed of components A, B, N, O (organic), and W (water). To simplify the equilibrium calculations, the following assumptions are made. Solutes A and B are soluble and miscible in solvents O and W. The adducting agent, N, is miscible and completely soluble in W, but is absent from the organic phase. Solvents O and W are completely immiscible. The following equilibrium reactions occur in W:

$$A + N \leftrightarrow A \cdot N \tag{27}$$

$$B + N \leftrightarrow B \cdot N. \tag{28}$$

The adducts are absent in O, and their solubility in W is calculated from Eq. 4. The physical parameters for this system are given in Table 5.

Under isothermal, isobaric conditions where one of the adducts precipitate, the system has two degrees of freedom. From the transformed phase diagram conditions are easily identified that lead to selective crystallization. Taking $A \cdot N$ and $B \cdot N$ as the reference components gives the following independent transforms:

Table 5. Parameters for Reactive Extractive Crystallization

$D_A = 30$	$x_{A\cdot N}^{sat} = 1 \times 10^{-2}$
$D_B = 60$	$x_{B\cdot N}^{sat} = 1 \times 10^{-3}$
$K1 = 1$	$K2 = 40$

where

$$D_A = \frac{x_{A,org}}{x_{A,aq}} \quad \text{and} \quad D_B = \frac{x_{B,org}}{x_{B,aq}}$$

$$X_B = \frac{x_B + x_{B\cdot N}}{1 + x_{A\cdot N} + x_{B\cdot N}} \tag{29}$$

$$X_N = \frac{x_N + x_{A\cdot N} + x_{B\cdot N}}{1 + x_{A\cdot N} + x_{B\cdot N}} \tag{31}$$

$$X_O = \frac{x_O}{1 + x_{A\cdot N} + x_{B\cdot N}} \tag{31}$$

$$X_W = \frac{x_W}{1 + x_{A\cdot N} + x_{B\cdot N}}. \tag{32}$$

Figure 10a is the transformed phase diagram plotted in terms of X_W, X_O. The $A\cdot N - B\cdot N$ saturation trough is given by the curve generated by the overlap between the $A\cdot N$ and $B\cdot N$ saturation surfaces and where the mole fractions of water are equal on both surfaces. Notice that even though W extracts A twice as well as B, the $B\cdot N$ saturation surface is much larger than the AN saturation surface due to a 40 times larger equilibrium constant for this reaction and the fact that the solubility of $B\cdot N$ is 10 times less than the solubility of $A\cdot N$.

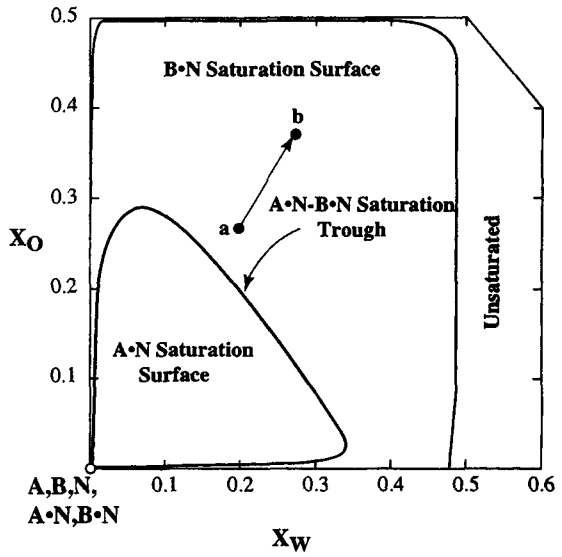

(a)

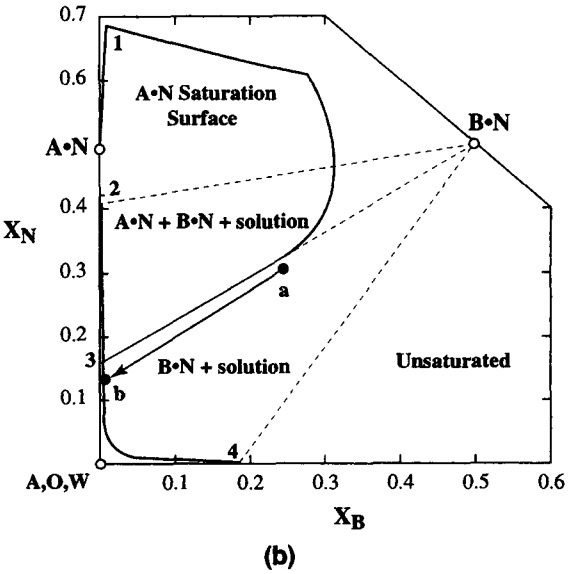

(b)

Figure 10. (a) Phase diagram for reactive extractive crystallization system; (b) another view of its phase diagram.

Figure 10b is the phase diagram of the same system, but plotted in terms of X_B and X_N. Region $A\cdot N13$ represents the $A\cdot N$ saturation surface. Curve 23 is the $A\cdot N-B\cdot N$ double-saturation trough. Curve 234 represents the side of the $B\cdot N$ saturation surface. Any composition within region $B\cdot N234$ that also lies on the $B\cdot N$ saturation surface in Figure 10a is supersaturated with respect to $B\cdot N$. For example, a composition at point a will equilibrate to a composition at point b by precipitating $B\cdot N$. Compositions within region $B\cdot N23$ that also lie on the $A\cdot N$ saturation surface in Figure 10a is supersaturated with respect to both $A\cdot N$ and $B\cdot N$, and will equilibrate to a composition on the $A\cdot N-B\cdot N$ double-saturation trough. Compositions within region $A\cdot N12$ that also lie on the $A\cdot N$ saturation surface in Figure 10a are supersaturated with $A\cdot N$.

Synthesis of Separation Processes

When the relative solubilities of the components in solution are strong functions of temperature and concentration, processes can be synthesized that use temperature, solvent, and pressure swings to completely separate a mixture into pure components.

Use of temperature and solvent swings

Compound formation has been proposed to separate many close-boiling species. For example, Figure 11 shows the phase diagram for acetic acid, quinaldine, and isoquinoline and a flow sheet to separate the components. Stream numbers in the flow sheet and points on the phase diagram correspond to one another. The feed is combined with the effluent from $C2$, stream (4), to make stream (1). The stream is cooled to T_1. Crystals of isoquinoline precipitate from solution and are then filtered from the process. The effluent, stream (2), is combined with the distillate to make stream (3). The stream is fed to $C2$, which operates at T_2. Crystals of the quinaldine · acetic acid adduct are filtered, remelted, and sent to a distillation column. Assuming that the quinaldine does not decompose, the bottom is composed of quinaldine at a specified purity. The distillate rich in acetic acid is recycled.

Use of temperature and solvent swings in a reactive system can sometimes be used to separate the pure components without having to crystallize a reaction product. Figure 12 shows phase diagrams where A and B react to form C in inert I and the flow sheet to obtain pure A and B. For simplicity, it is assumed that pure I can be evaporated or distilled from the system. Either pure A or B can be obtained at the first crystallizer, $C1$, while the second crystallizer, $C2$, recovers the other pure component. The process to remove A first proceeds as follows. The feed (F) and stream (5) are combined to make stream (1), which is combined with the I distilled from the crystallizer effluent. Stream (2) is fed into $C1$, which operates at T_1. The amount of solvent is I_1. Because the composition of the stream lies within the A saturation field at this temperature and solvent composition, com-

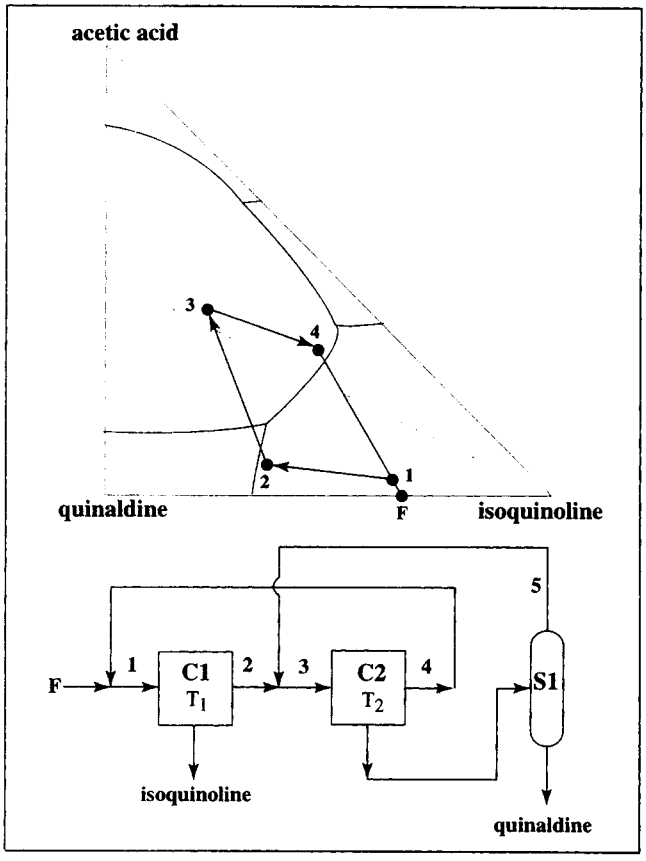

Figure 11. Process to separate quinaldine and isoquinoline.

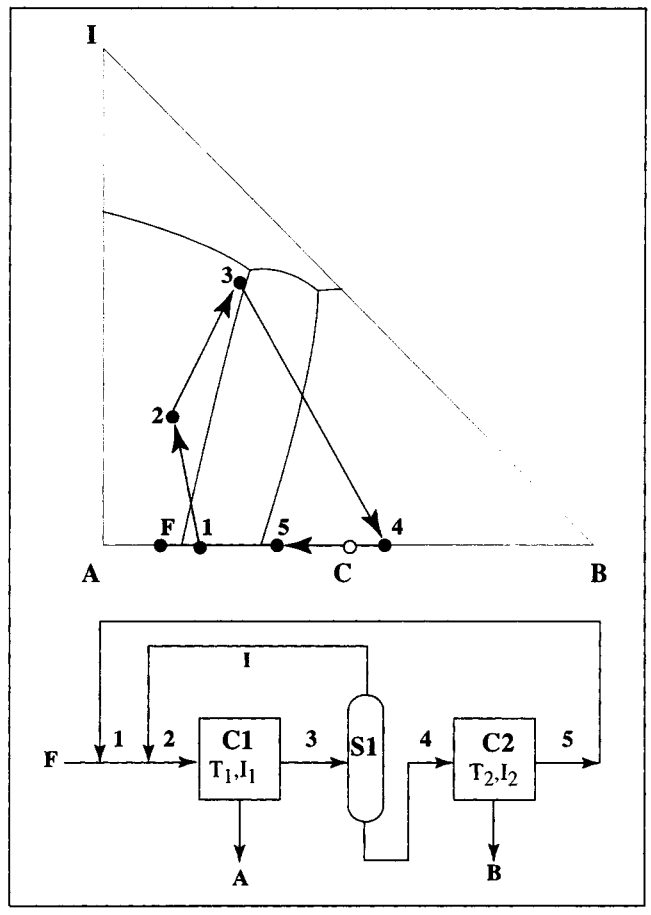

Figure 12. Process to separate *A* and *B* without crystallizing compound.

ponent A crystallizes from solution and is then filtered from the system. The crystallizer effluent, stream (3) is partially distilled of I in the distillation column. The bottoms are sent to $C2$, which operates at T_2 and at solvent level I_2. The composition of the system now lies in the B saturation field. B crystallizes and is filtered from the system. The crystallizer effluent is recycled. Notice that C must melt incongruently for the separation to work.

Use of temperature, pressure and solvent swings

The partial pressures of the components in solution can greatly impact crystallizer design. By choosing the appropriate reaction conditions, specific species can be made to selectively crystallize. For example, consider the following system of reactions:

$$A + B \leftrightarrow C\downarrow$$
$$C + D \leftrightarrow E\downarrow$$
$$C \leftrightarrow G\downarrow + H(\mathrm{g}) \tag{33}$$

where C, E, and G have limited solubility in the reaction mixture and H is a gas that is soluble in the reaction mixture. The partial pressure of H is much greater than the partial pressures of the other species in solution. At a specified temperature and pressure, there are $7(c)-3(p)-3(r)=1$ degree of freedom, and four transforms. Using C, E, and G as the reference components, two of the transformed coordinates are

$$X_A = \frac{x_A + x_C + x_E + x_G}{1 + x_C + 2x_E} \tag{34}$$

$$X_D = \frac{x_D + x_E}{1 + x_C + 2x_E}. \tag{35}$$

The input data for calculating the solubilities and equilibrium constants are given in Table 6. Figure 13a is the phase diagram at 310 K and at a partial pressure of H equal to 1 atm

Table 6. Parameters to Generate Multireaction Heterogeneous Phase Diagram in Figure 13

Reaction 1	$E1 = -12.125$	$E2 = 7{,}164.6$	$E3 = -8.0\times10^5$
Reaction 2	$E1 = 13.264$	$E2 = -3{,}314.8$	$E3 = 8.0\times10^4$
Reaction 3	$E1 = 0.671$	$E2 = 2{,}015.8$	$E3 = -6.0\times10^5$

	ΔH_m^0 (J/mol)	T_m (K)
C	20,756	650
E	17,917	640
F	3,253	630

where

$$\frac{\Delta G^0}{RT} = -E1 - \frac{E2}{T} - \frac{E3}{T^2}$$

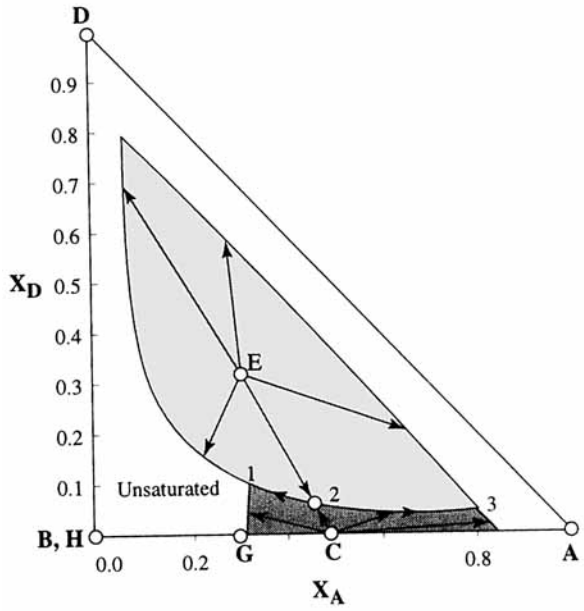

(a)

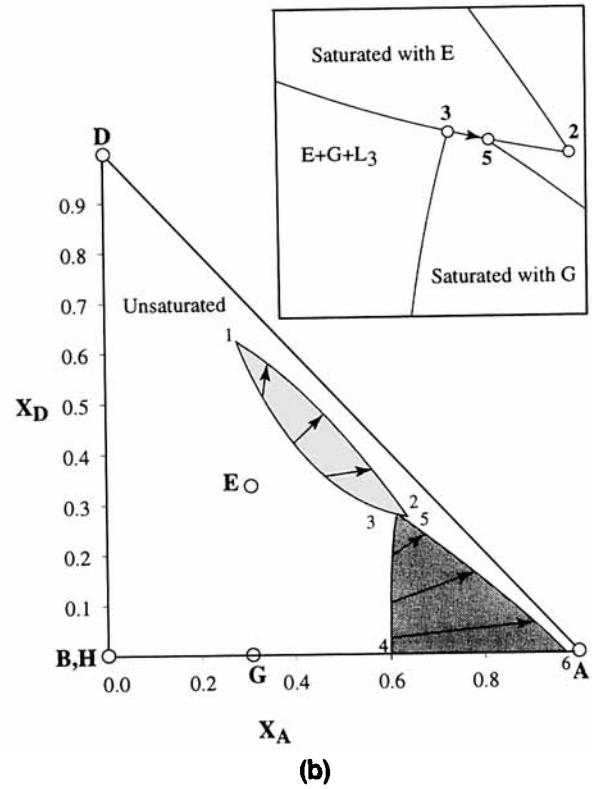

(b)

Figure 13. Phase diagram for a seven-component system with three reactions: (a) at T_1 and P_1; (b) at T_2 and P_2.

(T_1, P_1). The points representing the pure components are labeled on the plot. Compositions within the unshaded region remain unsaturated. Compositions within the lightly and darkly shaded regions are saturated with E and C, respectively. Several crystallization paths that describe the precipitation of E and C are drawn on the plot. Both E and C melt congruently. At this temperature and pressure, G does not crystallize. Points 1 and 3 are the solutions to where E and C cocrystallize. Point 2 is a saddle point where E and C continuously crystallize until the system dries up. Any mixture described by a point between points 1 and 2 on line 123 converges to a composition given by point 1. Any point on line 123 between points 2 and 3 converges to point 3.

Figure 13b is the phase diagram for the same system at 350 K and at partial pressure of H equal to 0.2 atm (T_2, P_2). Under these conditions only E and G can crystallize. Both components melt incongruently. The regions where E crystallizes is lightly shaded and is enclosed by points 1253. Curves 13 and 52 represent conditions where the solution is just saturated but crystallization does not occur. For a system to equilibrate on this curve, the system must have any initial composition on curve 13. Compositions on curve 35, but not at point 3, will cocrystallize E and G until reaching 5. All other compositions within region 1235 will crystallize E until reaching curve 12. The regions where G crystallizes is darkly shaded and is enclosed by points 3564. Curve 34 represents a saturated solution of G. Compositions within 3564 cause the crystallization of G until curve 56 is reached. All unshaded

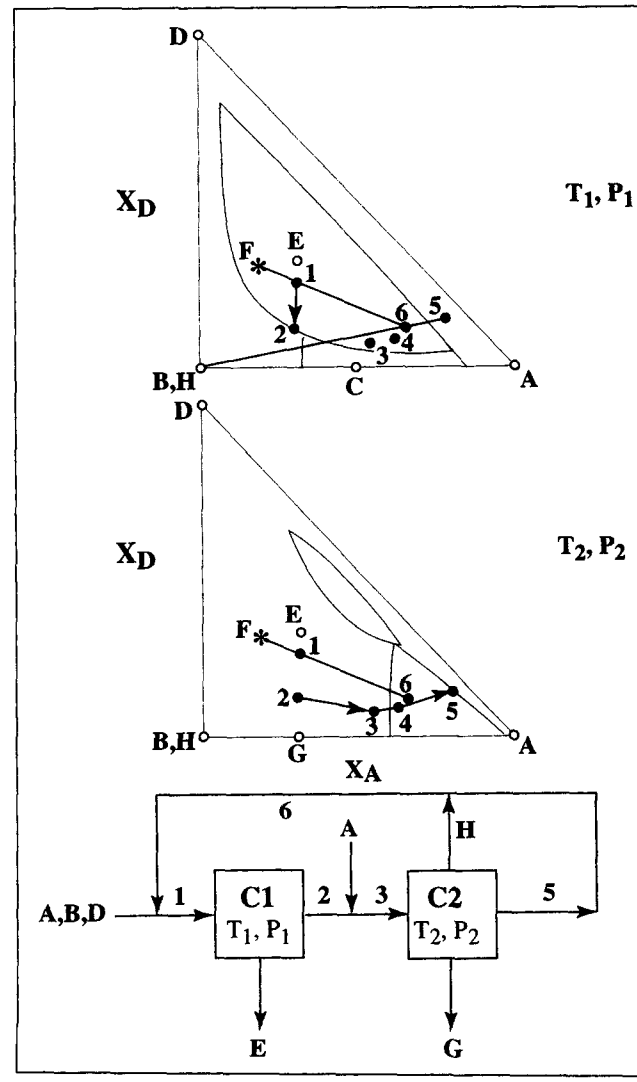

Figure 14. Process to crystallize E and G.

regions represent unsaturated solution. Crystallization paths for the crystallization of E and G are shown as arrows originating from the respective pure component.

By using these two-phase diagrams, separation cycles can be synthesized that recover any combination from C, E, and G. For example, Figure 14 shows a process to recover E and G. It begins by combining a feed (F) that is composed of A, B, and D with recycle (stream 6) to make stream (1). The stream is fed into a crystallizer ($C1$) that operates at T_1 and P_1. Component E crystallizes and is filtered from the system. The mother liquor is combined with a stream of pure A to make stream (3). The stream is sent to the second crystallizer ($C2$), which operates at T_2 and P_2 and vents H. Component G crystallizes and is filtered from the system. The mother liquor (stream 5) is recycled. It is assumed that H is also recycled along with the mother liquor, although using compressors and other practical issues need to be considered.

Figure 15 shows a process to separate solid C, E, and G. The feed, which consists of A and B, is combined with recycled H to make stream (1). Stream (1) is sent to $C1$, which operates at T_1 and P_1. Solid C is filtered from the system. The crystallizer effluent is combined with stream (9). More A is added and the stream is sent to $C2$, which operates at T_2 and P_2 and vents gaseous H. As a result of these conditions, G crystallizes, and it is filtered from the system. The mother liquor is combined with streams composed of B and D. The stream (8) is sent to $C3$, which operates at T_1 and P_1. The crystals of E are filtered and the mother liquor is recycled.

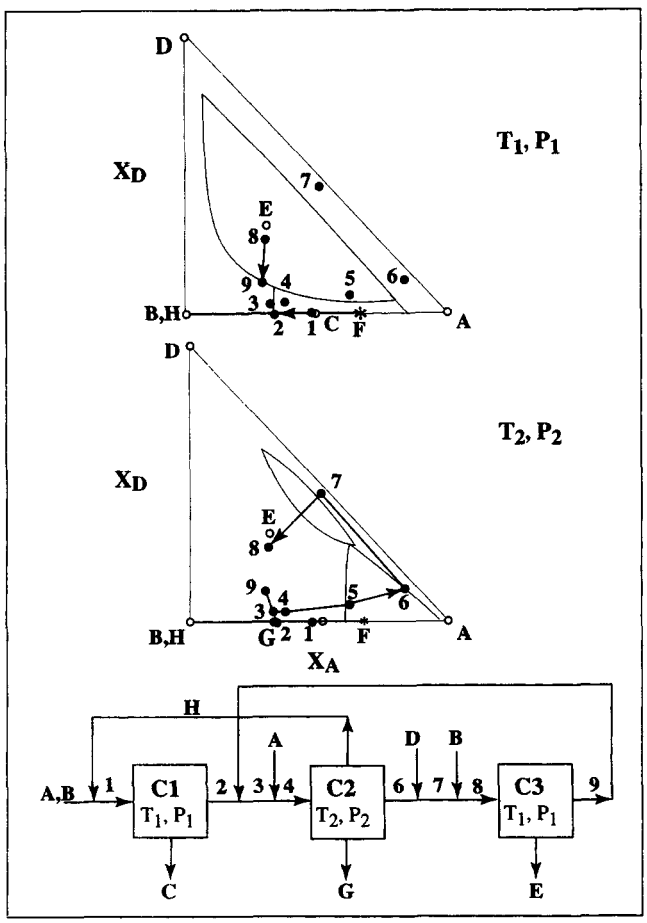

Figure 15. Process to crystallize C, E, and G.

Conclusions

A systematic method is presented to synthesize reactive crystallization processes. The article begins with a procedure for the calculation of solid–liquid phase diagrams for multicomponent systems. The species may undergo complex reactions in the liquid phase, and some of the reaction products may precipitate. While it is assumed that the solid phases are completely immiscible and that the liquid and solid phases are ideal in these examples, nonideality has been accounted for in the model.

If the resulting phase behavior is plotted with the traditional temperature-composition (e.g., mole fractions) diagrams, visualization of the behavior of the system would be severely limited, strictly speaking, to no more than three components. This problem is circumvented by using a set of transformed coordinates. Only compositions on a reaction surface are shown in this transformed coordinate system. This view can be further restricted to that on a saturation surface. Phase diagrams for systems with three or fewer degrees of freedom can be viewed in its entirety, regardless of the number of components and reactions. For systems with more than three degrees of freedom, the thermodynamic behavior is gleaned from sectional cuts of the high-dimensional phase diagram. All of these phase diagrams can be easily examined, thus providing a useful tool for process synthesis.

This method is illustrated with a wide variety of examples. These include systems with multiple reactions and multiple phases. Some examples show how to determine conditions under which the desired products can be recovered as crystals. Conversely, in the fourth example with six components, three phases, and two reactions, we showed how to avoid the precipitation of an undesirable byproduct because of the possible reaction between a species in the vapor and another in the liquid. Other examples demonstrate how to use compound formation, particularly adducts, to separate a mixture.

Process flow sheets are provided for some of these examples. These separation processes were synthesized by bypassing the thermodynamic barriers imposed on the system by the chemical reactions and the solubilities of the components in the mixture. By combining crystallizers with other unit operations, the stream compositions were driven to regions within composition space where selective crystallization could occur. Consider the example for the separation of isoquinoline and quinaldine using an acetic acid · quinaldine adduct. Isoquinoline is crystallized. By adding acetic acid, the system moves into a region where the adduct crystallizes. After removing the adduct and distilling acetic acid, the system is driven back to a region where isoquinoline can crystallize. Other possible separation schemes can be similarly synthesized.

This study provides the necessary framework for the design of reactive crystallization processes. In general, data for crystallization, let alone reactive crystallization, may not be readily available. It is for this reason that we primarily used hypothetical examples. A wide variety of experimental techniques are available for the determination of solubility and solid–fluid behavior in general (Myerson, 1993). However, these experiments tend to be time-consuming. To expedite

the development of crystallization processes, the procedure suggested in this study can be used to determine what data are needed and the region of composition space where the experimental efforts should be focused.

Acknowledgment

We express our appreciation to the National Science Foundation for support of this research (Grant No. CTS-9220196).

Notation

P = pressure
S = distillation column
x = liquid-phase mole fraction
X = transformed coordinate
ξ = extent of reaction

Subscripts and superscripts

i,j,k = index
0 = initial condition

Literature Cited

Åslund, B. L., and Å. C. Rasmuson, "Semibatch Reaction Crystallization of Benzoic Acid," *AIChE J.*, **38**, 328 (1992).
Bailey, W. A., R. A. Bannerot, L. C. Fetterly, and A. G. Smith, "Urea Extractive Crystallization of Straight Chain Hydrocarbons," *Ind. Eng. Chem.*, **43**, 2125 (1951).
Bemis, A. G., J. A. Dindorf, B. Horwood, and C. Samans, "Phthalic Acids," *Kirk Othmer Encyclopedia of Chemical Technology*, Vol. 17, 3rd ed., Wiley, New York, p. 732 (1982).
Berry, D. A., and K. M. Ng, "Separation of Quaternary Conjugate Salt Systems by Fractional Crystallization," *AIChE J.*, **42**, 2162 (1996).
Berry, D. A., S. R. Dye, and K. M. Ng, "Synthesis of Drowning-out Crystallization-based Separations," *AIChE J.*, **43**, 91 (1997).
Dale, G. H., "Crystallization, Extractive and Adductive," *Encycl. Chem. Process Des.*, **13**, 456 (1981).
Dye, S. R., and K. M. Ng., "Bypassing Eutectics with Extractive Crystallization: Design Alternatives and Trade-Offs," *AIChE J.*, **41**, 1456 (1995a).
Dye, S. R., and K. M. Ng, "Fractional Crystallization: Design Alternatives and Trade-offs," *AIChE J.*, **41**, 2427 (1995b).
Franke, J., and A. Mersmann, "The Influence of the Operational Conditions on the Precipitation Process," *Chem. Eng. Sci.*, **50**, 1737 (1995).
Franck, R., R. David, J. Villermaux, and J. P. Klein, "Crystallization and Precipitation Engineering—II. A Chemical Reaction Engineering Approach to Salicylic Acid Precipitation: Modeling of Batch Kinetics and Application to Continuous Operation," *Chem. Eng. Sci.*, **43**, 69 (1988).
Gaikar, V. G., and M. M. Sharma, "Dissociation Extractive Crystallization," *Ind. Eng. Chem. Res.*, **26**, 1045 (1987).
Gaikar, V. G., A. Mahapatra, and M. M. Sharma, "Separation of Close Boiling Point Mixtures (p-Cresol/m-Cresol, Guaiacol/Alkylphenols, 3-Picoline/4-Picoline, Substituted Anilines) through Dissociation Extractive Crystallization," *Ind. Eng. Chem. Res.*, **28**, 199 (1989).
Hilgeman, F. R., F. Y. N. Mouroux, D. Mok, and M. K. Holan, "Phase Diagrams of Binary Solid Azole Systems," *J. Chem. Eng. Data*, **34**, 220 (1989).
Jadhav, V. K., M. R. Chivate, and N. S. Tavare, "Separation of p-Cresol from its Mixtures with 2,6-Xylenol by Adductive Crystallization," *J. Chem. Eng. Data*, **36**, 249 (1991).
Jadhav, V. K., M. R. Chivate, and N. S. Tavare, "Separation of Phenol from its Mixtures with o-Cresol by Adductive Crystallization," *J. Chem. Eng. Data*, **37**, 232 (1992).
Kennard, S. M., and P. A. McCusker, "Some Systems of Carbon Halides with Dioxane, Pyridine, and Cyclohexane," *J. Amer. Chem. Soc.*, **70**, 3375 (1948).
Lahti, L. E., and F. S. Manning, "Initial Kinetic Study of Urea Adduction with n-Octane, n-Decane, and n-Dodecane," *Ind. Eng. Chem. Process Des. Dev.*, **4**, 254 (1965).
Lencka, M. M., and R. E. Riman, "Thermodynamic Modeling of Hydrothermal Synthesis of Ceramic Powders," *Chem. Mater.*, **5**, 61 (1993).
Malesinski, W., *Azeotropy and Other Theoretical Problems of Vapour-Liquid Equilibrium*, Interscience, New York (1965).
Marcant, B., and R. David, "Experimental Evidence for and Prediction of Micromixing Effects in Precipitation," *AIChE J.*, **37**, 1698 (1991).
McCandless, F. P., R. D. Mountain, R. D. Olan, S. P. Roth, and L. J. Van Dyke, "Separation of Trimethylpentanes by Extractive Crystallization with Thiourea," *Ind. Eng. Chem., Prod. Res. Dev.*, **11**, 463 (1972).
McCandless, F. P., and E. L. Handl, "Separation of β-Phellandrene from Dipentene by Extractive Crystallization with Thiourea," *Ind. Eng. Chem., Prod. Res. Dev.*, **12**, 132 (1973).
McCrary, A. L., and W. L. Howard, "Chelating Agents," *Kirk Othmer Encyclopedia of Chemical Technology*, Vol. 5, 3rd ed., Wiley, New York, p. 339 (1979).
Mendiratta, A. K., "Ion Exchange Catalyzed Bisphenol Process," U.S. Patent, 4,391,997 (1983).
Mersmann, A., and M. Kind, "Chemical Engineering Aspects of Precipitation from Solution," *Chem. Eng. Tech.*, **11**, 264 (1988).
Momomaga, M., H. Yazawa, and K. Kagara, "Reactive Crystallization of Methyl α-Methoxyimino Acetoacetate," *J. Chem. Eng. Japan*, **25**, 237 (1992).
Prausnitz, J. M., R. N. Lichtenthaler, and E. G. Azevedo, *Molecular Thermodynamics of Fluid-Phase Equilibria*, Prentice Hall, Englewood Cliffs, NJ (1986).
Myerson, A. S., ed., *Handbook of Industrial Crystallization*, Butterworth-Heinemann, Boston (1993).
Rajagopal, S., K. M. Ng, and J. M. Douglas, "Design of Solids Processes: Production of Potash," *Ind. Eng. Chem. Res..*, **27**, 2071 (1988).
Rajagopal, S., K. M. Ng, and J. M. Douglas, "Design and Economic Trade-offs of Extractive Crystallization Processes," *AIChE J.*, **37**, 437 (1991).
Schiek, R. C., "Pigments, Inorganic," *Kirk Othmer Encyclopedia of Chemical Technology*, Vol. 17, 3rd ed., Wiley, New York, p. 788 (1982).
Slaughter, D. W., and M. F. Doherty, "Calculation of Solid-Liquid Equilibrium and Crystallization Paths for Melt Crystallization Processes," *Chem. Eng. Sci.*, **50**, 1679 (1995).
Smith, W. R., and R. W. Missen, *Chemical Reaction Equilibrium Analysis: Theory and Algorithms*, Wiley-Interscience, New York (1982).
Söhnel, O., "Chemical Design of Precipitation Processes," *Advances in Industrial Crystallization*, J. Garside, R. J. Davey, and A. G. Jones, eds., Butterworth-Heinemann, Boston (1991).
Söhnel, O., and J. Garside, *Precipitation: Basic Principles and Industrial Applications*, Butterworth-Heinemann, Boston (1992).
Tare, J. P., and M. R. Chivate, "Selection of a Solvent for Adductive Crystallization," *Chem. Eng. Sci.*, **31**, 893 (1976a).
Tare, J. P., and M. R. Chivate, "Separation of Close Boiling Isomers by Adductive and Extractive Crystallization," *AIChE Symp. Ser. No. 153*, **72**, 95 (1976b).
Tavare, N. S., *Industrial Crystallization Process Simulation and Design*, Plenum Press, New York (1995).
Tavare, N. S., and V. G. Gaikar, "Precipitation of Salicylic Acid: Hydrotropy and Reaction," *Ind. Eng. Chem. Res.*, **30**, 722 (1991).
Toyokura, K., K. Tawa, and J. Ueno, "Reaction Crystallization of Sulfamic Acid from Urea and Fuming Sulfuric Acid," *J. Chem. Eng. Japan*, **12**, 24 (1979).
Tyner, M., "Enthalpy-Concentration Diagrams of Binary Aqueous Mixtures of Hydrazine, Sodium Carbonate, and Glycerine," *AIChE J.*, **1** 87 (1955).
Ung, S., and M. F. Doherty, "Vapor-Liquid Phase Equilibrium in Systems with Multiple Chemical Reactions," *Chem. Eng. Sci.*, **50**, 23 (1995).

Manuscript received Nov. 4, 1996, and revision received Mar. 3, 1997.